J. theor. Biol. (1997) **185,** 263–280

Effects of Inhibition on Neural Network Development Through Activity-dependent Neurite Outgrowth

C. van Oss and A. van Ooyen*

Netherlands Institute for Brain Research, Meibergdreef 33, 1105 *AZ Amsterdam, The Netherlands*

(*Received on* 28 *September* 1995, *Accepted in revised form on* 6 *December* 1996)

Empirical studies have demonstrated that electrical activity of the neuron can directly affect the outgrowth of its neurites. In this paper, the implications of activity-dependent neurite outgrowth are studied in a simple two-cell model, containing one excitatory and one inhibitory cell. We show that activity-dependent outgrowth in combination with the presence of inhibition can account for bistability. The attractors, which can be both point and limit cycle attractors, may be associated with "normal" and "pathological" end states of network development. A slight modification of the model makes it applicable also to a range of other activity-dependent processes in neurons, such as changes in the number or efficacy of receptors. The main results of the previous model are also found in the modified model.

1. Introduction

During development, as neurons become assembled into functioning networks, many processes that determine network structure and function are affected by the neuron's electrical activity [for reviews see Fields & Nelson, (1992); and van Ooyen (1994)]. Intrinsically generated electrical discharges and synaptic interactions are especially important in this respect during the primary phases of network development (Corner, 1994). As a result of such activity-dependent processes, a reciprocal influence or feedback loop becomes established between the development of neuronal form, function and connectivity on the one hand, and network activity on the other hand. A given network may generate activity patterns which modify the organization of the network, leading to altered activity patterns which could further modify structural or functional characteristics, and so on. A developing network is thus a dynamic system in which the structure, number of elements, and functional characteristics of the elements are variable, in part being under the influence of the system's own activity. The presence of such feedback loops has implications not only for the emergence of network organization and function, but also for the functioning of the mature system: processes that are involved in development often appear to remain operative in adulthood [for references see van Ooyen (1994)]. In this paper, we address the implications of two of these activity-dependent processes, namely neurite outgrowth and receptor adaptation.

A number of studies have demonstrated that the neuron's electrical activity affects, presumably via changes in intracellular calcium levels, the outgrowth of its neurites, with high levels of activity (resulting in high intracellular calcium concentrations) causing neurites to retract, whereas low levels of activity and, consequently, low intracellular calcium allow further outgrowth (Cohan & Kater, 1986; Mattson, 1988; Kater *et al*., 1990). From these studies, the realization is growing that electrical activity is not only involved in information coding, but may also play an important role in shaping neuronal form and network structure (Mattson, 1988). By means of simulation

* Author to whom correspondence should be addressed.

0022–5193/97/060263 + 18 $25.00/0/jt960361

models, we tried to make this more explicit. We previously demonstrated that such activity-dependent neurite outgrowth in a purely excitatory neural network model can, under a wide range of conditions, give rise to a transient phase during development in which the connectivity is larger than in the final, stable state (van Ooyen & van Pelt, 1994). The essential condition for the occurrence of such an "overshoot" is a hysteresis relation between network activity and connectivity, which in the model is attained by the firing threshold in the neuronal response function. Overshoot phenomena with respect to many structural elements (e.g., the number of synapses) constitute a widespread feature of nervous system development, *in vivo* as well as *in vitro* [for references see van Ooyen & van Pelt (1994)].

We have also studied networks made up of both excitatory and inhibitory cells (van Ooyen *et al*., 1995; throughout this paper, this model will be referred to as the "network model"), and in such mixed networks overshoot still takes place. New is, however, that the "basin of attraction" of the attractor of the system is diminished as a consequence of inhibition. In other words, whereas purely excitatory networks end up in the same attractor regardless of initial conditions, mixed networks do not necessarily do so. In a mixed network with a moderate level of inhibition and an initial average connection strength that is larger than a critical value, connectivity will not be reduced but, instead, will continue to increase (the studied network in (van Ooyen *et al*., 1995) was not found to end up in a second attractor, see Discussion). Similar phenomenona have been observed in developing cultures of dissociated cortex cells with respect to the number of synapses. Cultures developing under normal conditions show a transient overproduction of synapses, i.e., overshoot, with an initial period of neurite outgrowth and synapse formation being followed by a period of substantial synapse elimination towards a stable level (van Huizen, 1986; van Huizen *et al*., 1987a; van Huizen *et al*., 1985). In contrast, a developing culture that is chronically deprived of electrical activity (thus resulting in enhanced neurite outgrowth with no subsequent elimination of synapses) for longer than a certain period, does not eliminate its excess synapses when electrical activity is allowed to return (van Huizen *et al*., 1987b). This observation has been taken to indicate that there may exist a "critical", or "sensitive", period after which electrically controlled pruning of connections is no longer possible.

The aim of the present paper is to better understand the phenomenon of such critical periods, and to pinpoint the interactions that may be important for its existence. To this end the network model (van Ooyen *et al*., 1995), which contains a large number of spatially distributed cells, is greatly simplified. The first simplification is the exclusion of the spatial dimension. Secondly, the number of neurons is reduced to two, where, since the presence of inhibition was found to be crucial for the existence of critical periods in the network model, one of them is taken to be inhibitory. A first attempt to analyse this simplified model has been made in (van Ooyen *et al*., 1995). The results suggested that the end state of the network is dependent on initial conditions and that, therefore, the phenomenon of a critical period could exist in this simple model. This could not be tested explicitly, however, since activity-dependent neurite outgrowth was not explicitly included in this simplification. In this paper, we therefore introduce activity-dependent neurite outgrowth to the simplified model. For simplicity, at first only the excitatory cell is allowed to adapt its neurites, whereas those of the inhibitory cell are held constant. Focusing on the possible existence of multistability, we analyse the complete dynamic behaviour generated by this model. In addition, we make a start at analysing an extended model in which the neurites of both cells are variable.

Besides neurite outgrowth, many other processes that are important in determining the structure and function of the nervous system are activity-dependent to a certain degree. With a slight modification of the model, it also applies to a range of other activity-dependent processes, such as changes in receptor number or efficacy. The main results of the previous models are also found in this model, which underlines the generality of the findings.

Preliminary results of this study have been reported in (van Oss & van Ooyen, 1995).

2. The Model

The shunting model of Grossberg (1988) is used for describing neuronal activity. Here the dimensionless equations (Carpenter & Grossberg, 1983; van Ooyen *et al*., 1995) are used. In this model, excitatory inputs drive the membrane potential towards a finite maximum (or saturation potential, e.g., the Na^+ equilibrium potential), while inhibitory inputs drive the membrane potential towards a finite minimum (e.g., the K^+ equilibrium potential). The general form of these equations is:

$$\begin{aligned}\frac{dx}{dt} &= -x + (1-x)w_{xx}f(x) - (h+x)w_{xy}f(y)\\ \frac{dy}{dt} &= -y + (1-y)w_{yx}f(x) - (h+y)w_{yy}f(y),\end{aligned} \tag{1}$$

where x represents the time averaged membrane potential of the excitatory cell, y that of the inhibitory cell ($x, y \epsilon \langle -h, 1 \rangle$), w_{xx}, w_{xy}, w_{yx} and w_{yy} are the connection strengths of cell x to x, y to x, x to y and y to y, respectively (all $w \geqslant 0$). We thus model a single excitatory cell that is connected to itself (with strength w_{xx}), which can be interpreted as a simplification for modelling two completely identical and reciprocally coupled excitatory cells. An alternative interpretation of eqn (1) is that x and y represent the average membrane potential of a population of excitatory and inhibitory neurons, respectively [see Wilson & Cowan (1972)]. For simplicity, we exclude mutual inhibition ($w_{yy} = 0$) and assume that the connection between the excitatory and inhibitory unit is symmetrical ($w_{yx} = w_{xy}$). This last assumption is relaxed in Section 5. The output of the cells is their mean firing rate f, which is taken to be a sigmoidal function of the membrane potential u:

$$f(u) = \frac{1}{1 + e^{(\theta - u)/\alpha}},$$

where α determines the steepness of the function, while θ represents the firing threshold. The low firing rate when the membrane potential is sub-threshold may be considered as representing spontaneous activity, arising from threshold or membrane potential fluctuations and synaptic noise.

For modelling neurites we use the concept of a neuritic field with radius R, as yet without distinguishing axons and dendrites (but see Section 5). The size of the neuritic fields of the cells is governed by the following equations ($R_x > 0$ and $R_y > 0$):

$$\frac{dR_x}{dt} = q^*(\epsilon - g(R_x) - x) \tag{2}$$

$$\frac{dR_y}{dt} = q^*(\epsilon - g(R_y) - y),$$

where R_x is the size of the neuritic field of cell x, R_y is the size of the neuritic field of cell y, q^* is the growth rate of R_x and R_y, and ϵ, together with $g(R_u)$, determines the membrane potential u at which $dR_u/dt = 0$. To prevent the neurites ever from growing out indefinitely (when u for some reason continues to remain low) the saturation term $-g(R_u)$ was added (without this saturation term, however, the model gives quite similar results: see Discussion). Function g should have the property that it has relatively little effect when R_u is small and has a significant effect when R_u is large. We choose:

$$g(R_u) = b^* R_u^2 \tag{3}$$

where b^* determines the degree of saturation. The change in size of the neuritic field of a cell thus depends on its membrane potential u: if $u < (\epsilon - b^* R_u^2)$, the cell's neuritic field will increase, whereas it will decrease, if $u > (\epsilon - b^* R_u^2)$. This is a phenomenological description of the empirical results obtained by (Kater *et al.*, 1990) (see Introduction). If $u = (\epsilon - b^* R_u^2)$, the neuritic field size will not change.

If we interpret x and y as representing the average membrane potential of populations of cells, R_x and R_y are the average neuritic field size of the population of excitatory and inhibitory cells, respectively.

If a cell's neuritic field increases, it is reasonable to assume that its connection strength with the other cells (both excitatory and inhibitory) increases. For the connection strengths between the cells we have

$$w_{xx} = \varphi(R_x) S_{xx} \tag{4}$$

$$w_{xy} = \psi(R_x, R_y) S_{xy},$$

where φ and ψ can be interpreted as functions relating neuritic field sizes with the number of connections (synapses) that can be made between cell x and x, and between cell x and y, respectively, while S_{xx} and S_{xy} represent the average synaptic strength of these connections, respectively ($S_{xx} > 0$ and $S_{xy} > 0$). Since we are interested in a simple model that still captures the essentials for generating the phenomena observed in the network model, we take R_y to be constant (in Section 4 this constraint is relaxed) and take simple functions φ and ψ: $\varphi(R_x) = aR_x$ and $\psi(R_x, R_y) = cR_x$ with $a, c > 0$. Using eqns (1) and (2) and $dw_{xx}/dt = S_{xx} a (dR_x/dt)$ yields

$$\frac{dx}{dt} = -x + (1 - x) w f(x) - (h + x) w p f(y)$$

$$\frac{dy}{dt} = -y + (1 - y) w p f(x) \tag{5}$$

$$\frac{dw}{dt} = q(\epsilon - b w^2 - x),$$

where

$$w = w_{xx}$$

$$p = (cS_{xy})/(aS_{xx}) = w_{xy}/w_{xx}$$

$$q = aS_{xx} q^*$$

$$b = b^*/(a^2 S_{xx}^2).$$

Throughout this paper, the model defined by eqn (5) will be called the "basic model". This model and those outlined in Section 4 and 5 are analysed using phase plane and bifurcation analysis, for which

we used the computer programs GRIND (De Boer, 1983) and LOCBIF (Khibnik *et al*., 1992).

Outgrowth of neurons is on a time-scale of days, so that connectivity is quasi-stationary on the time-scale of membrane potential dynamics (i.e., q is small). To avoid unnecessarily slowing down the simulations, q is chosen as large as possible while maintaining the quasi-stationary approximation. We use $q = 5{\cdot}10^{-3}$. In combination with an excitatory saturation potential of one, we choose $h = 0.1$, since the (absolute) value of the inhibitory saturation potential is usually about ten times smaller (e.g., Hodgkin & Huxley, 1952). As nominal values for the other parameters, we choose: $\theta = 0.5$, $\alpha = 0.1$, and $b = 5{\cdot}10^{-5}$, unless mentioned otherwise. The effect of other b and q values is discussed (see Discussion). The parameters ϵ and p vary from 0 to 1; their exact values are denoted in the figures.

3. Results

Since $q \ll 1$, the dynamics of w is much slower than that of x and y. Thus w can be considered as a slowly varying parameter, with x and y at quasi-steady state on the time-scale of w. Depending on the value of w, x and y can be either in a stable equilibrium (steady activity level) or in a limit cycle (oscillatory activity). Meanwhile, w may slowly change. Except for transient jumps, the trajectories of the system will either follow (if x and y are at equilibrium) or circle around (if x and y are in a limit cycle) the "slow manifold", this being the set of points for which $\mathrm{d}x/\mathrm{d}t = 0$ and $\mathrm{d}y/\mathrm{d}t = 0$. Intersections of the slow manifold with the nullcline of w (which is the set of points defined by $\mathrm{d}w/\mathrm{d}t = 0$) are the equilibrium points of the whole system (see Fig. 2). By using the concept of a slow manifold, the dynamics of the model can easily be displayed in the (w, x)- or (w, y)-plane.

We are interested in the impact of the parameters ϵ and p on the dynamic behaviour of the network. Parameter ϵ determines the membrane potential at which the neuron neither extends nor retracts its neurites, while p stands for the relative strength of the inhibitory connection, being $(cS_{xy})/(aS_{xx}) = w_{xy}/w_{xx}$. By means of bifurcation analysis it is possible to distinguish different regions in the parameter plane (ϵ, p) (see Fig. 1) and to characterize them in terms of number and stability of equilibrium points. The plane can be divided by fold and Hopf lines. A fold line consists of points at which a fold bifurcation (=saddle-node bifurcation) occurs. Crossing such a line due to a small change in ϵ or p means that two equilibrium points appear or disappear. A Hopf line consists of points at which a Hopf bifurcation occurs. Crossing such a line indicates that the stability of an equilibrium point has changed, and that stable or unstable limit cycles may appear or disappear. In our system, after careful examination of the (ϵ, p) parameter space and the (w, x) phase space for many (ϵ, p) combinations, we found only Hopf and fold bifurcations; no other co-dimension 1 bifurcations were found. Therefore, we consider it reasonable to assume that the number and stability of equilibria at every point in the parameter space is known once all Hopf and fold lines are found. A collection of points bounded by these lines is called a parameter region, which, as stated above, we assume to be homogeneous with respect to the number and stability of equilibrium points (but not necessarily so with respect to the existence of stable or unstable limit cycles). Table 1 gives an overview of all regions in the parameter plane of Fig. 1. In the model, three types of limit cycles are found; these will be explained in the following sections. The existence of a specific type of limit cycle could not always be excluded within a particular parameter region. In the following, only the parameter regions showing the most interesting behaviour will be described. A summary of the results will be given in Section 3.1.

PARAMETER REGIONS 1A, 2A AND 3: ONE ATTRACTOR

At low values of p the behaviour of the model is qualitatively the same as that of the model without inhibition. Figure 2(a) shows the (w, x)-plane at $p = 0.3$ and $\epsilon = 0.1$. The slow manifold is S-shaped ("hysteresis curve"), and there is only one equilibrium point. The nullcline of w, and consequently the position of the equilibrium point, can be shifted vertically by varying ϵ. This corresponds to a walk through the parameter plane with constant p and varying ϵ. In parameter region 1 ($0 < \epsilon < 0.12$) there is only one stable equilibrium, which is at the branch AB of the slow manifold. Region 2 is at intermediate ϵ values ($0.12 < \epsilon < 0.54$), for which there is one unstable equilibrium at the branch BC of the slow manifold, which gives a stable limit cycle ["relaxation oscillations", see e.g., Edelstein-Keshet (1988)], see Fig. 2(b–d). We will call this a "type 1" limit cycle. In region 3 ($0.54 < \epsilon < 1$) there is one stable equilibrium at branch CD. A trajectory starting at $w = 0$ will first follow branch AB, jump to CD and then approach the equilibrium point [Fig. 2(e)]. The trajectory therefore shows a transient overproduction in w [overshoot, see Fig. 2(f)]. Overshoot can occur if $\epsilon > 0.5$ and $p < 0.42$, thus in parameter regions 3, 5a, 5b, 6 and 7.

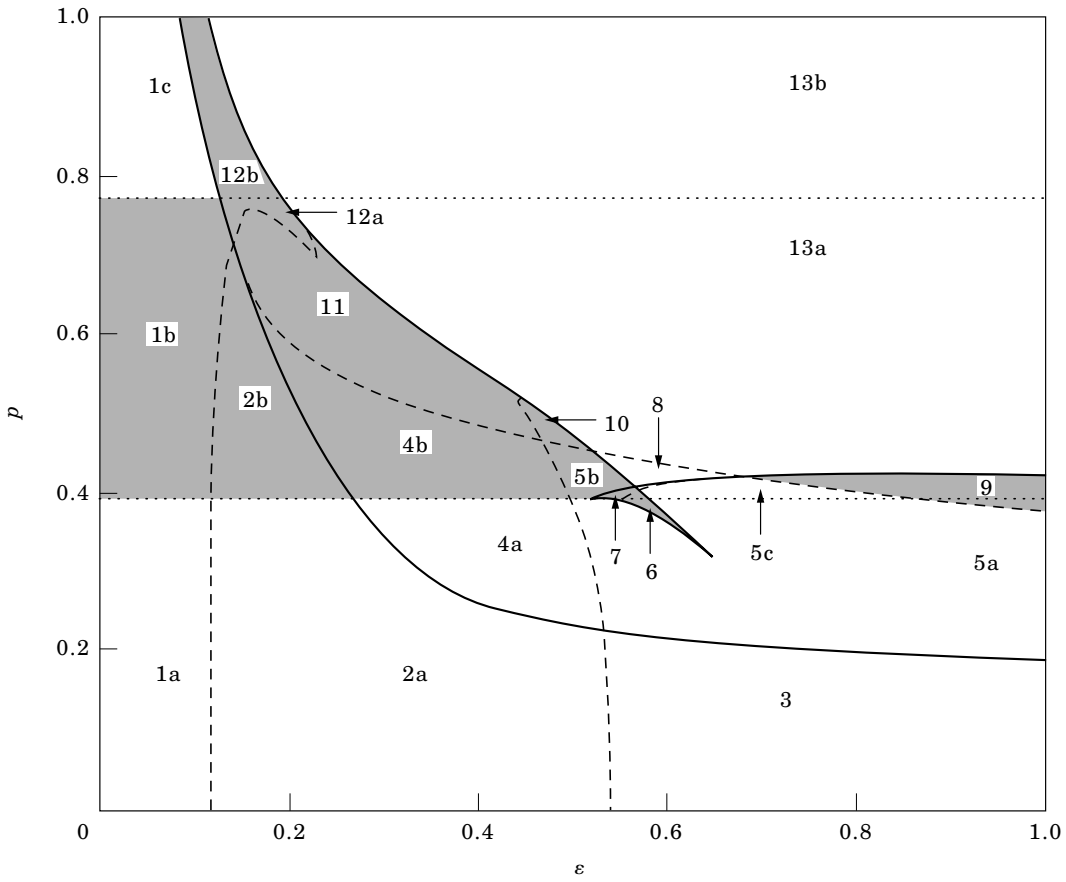

FIG. 1. Parameter plane p vs. ϵ. Within the area delineated by the two horizontal dotted lines an oscillatory state for x and y can exist for a fixed w. The continuous lines are fold lines, and the dashed lines are Hopf lines. Number and stability of equilibrium points and limit cycles in each numbered region are denoted in Table 1. The grey regions are those where two attractors can exist (i.e., bistability). For further details see text.

PARAMETER REGIONS 6, 9, 10 AND 12: TWO POINT ATTRACTORS

When p is increased, the slow manifold changes shape (Fig. 3) due to a cusp bifurcation at $p \approx 0.394$ and $\epsilon \approx 0.524$ (see Fig. 1). In parameter region 6, there are five equilibria, of which number 1 and 3 are stable (point attractors, see Fig. 3), and 2, 4 and 5 unstable (4 and 5 are not shown in Fig. 3). Two point attractors are also found in regions 9, 10 and 12.

PARAMETER REGIONS 5B, 7 AND 11: ONE POINT ATTRACTOR, ONE LIMIT CYCLE ATTRACTOR OF TYPE 2

In region 5 there are three equilibrium points, one stable and two unstable [see Fig. 4(a); one unstable equilibrium point is not shown]. In addition to the point attractor there is another attractor in the system, namely a stable limit cycle [Fig. 4(b–d)]. This limit cycle can be viewed as a switching between two states. Let us, for the moment, assume w to be a parameter rather than a variable. At $w = w_{fold}$, a fold bifurcation occurs whereby a saddle and a stable node appear (in the case of Fig. 4, $w_{fold} \approx 17.7$). At $w < w_{fold}$, x and y oscillate, whereas at $w > w_{fold}$, x and y are in a stable equilibrium. At $w = w_{fold}$, the limit cycle glues with the stable manifold of the newly appeared saddle node (i.e., a homoclinic bifurcation). A very slight increase in w causes the trajectory to move via the unstable manifold of the saddle to the stable node. Let us now consider the full system again, where changes in w are dependent on x: $dw/dt > 0$ when $x < (\epsilon - bw^2)$, and $dw/dt < 0$ when $x > (\epsilon - bw^2)$. In the (w, x)-plane this means that w increases below, and decreases above the w-nullcline. At $w < w_{fold}$, x and y oscillate and, on average, $x < (\epsilon - bw^2)$, as a result of which w will increase. At $w > w_{fold}$, on the other hand, x and y have a steady activity level whereby $x > (\epsilon - bw^2)$, so that w again decreases. Thus, w pulls the system back and forth through the homoclinic bifurcation. The limit cycle is stable, since w increases when $w < w_{fold}$, and decreases when $w > w_{fold}$. This type of oscillations, which in this paper will be denoted as a "type 2" limit cycle,

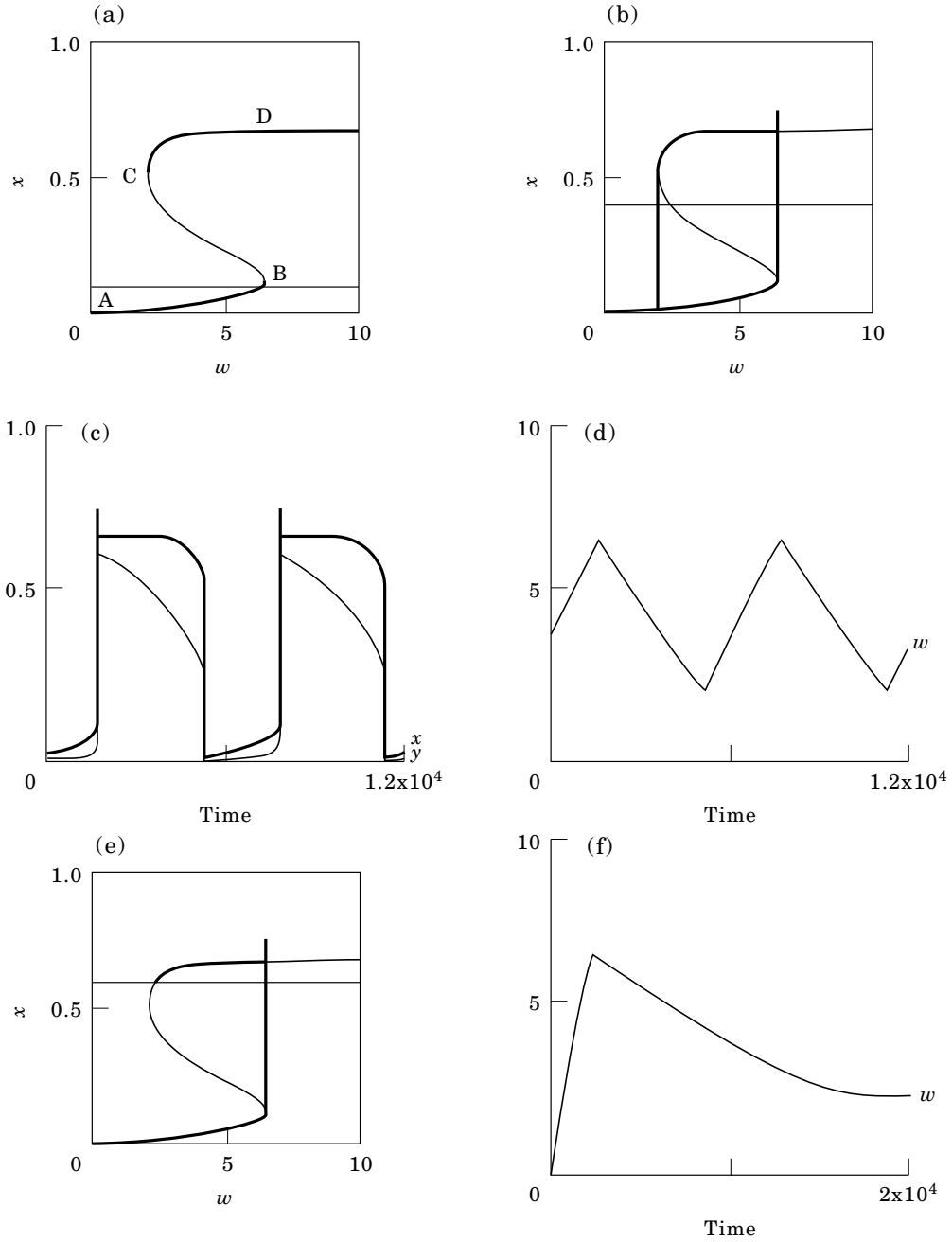

FIG. 2. (a) Parameter region la. The S-shaped slow manifold and the w-nullcline (thin, nearly horizontal line) in the (w, x)-plane. $p = 0.3$, $\epsilon = 0.1$. The bold lines of the slow manifold indicate stable equilibrium points with respect to x and y (when w is regarded as a parameter), and the thin lines unstable ones. Intersections of the slow manifold with the w-nullcline are the equilibrium points of the system. (b) $p = 0.3$, $\epsilon = 0.4$. The slow manifold (without showing stability) and the w-nullcline in the (w, x)-plane. The bold line is a trajectory following a limit cycle of type 1. (c) Time plot of the limit cycle attractor in (b) showing x (bold line) and y. (d) Time plot of the limit cycle attractor in (b) showing w. (e) $p = 0.3$, $\epsilon = 0.6$. The slow manifold (without showing stability) and the w-nullcline in the (w, x)-plane. The bold line is a trajectory showing overshoot in w. (f) Time plot of w of the trajectory in (e).

is known as "bursting oscillations" (Rinzel & Ermentrout, 1989).

The period of the limit cycle can be changed by varying ϵ. A smaller ϵ results in a longer period in region 2b and 11, and a shorter period in the other regions (the phase with steady activity becomes shorter). Only in region 2b and 11 is the dynamic behaviour of the type 2 limit cycle dependent on q, the parameter determining the growth rate. With a smaller q (i.e., slower dynamics of w), x and y, which

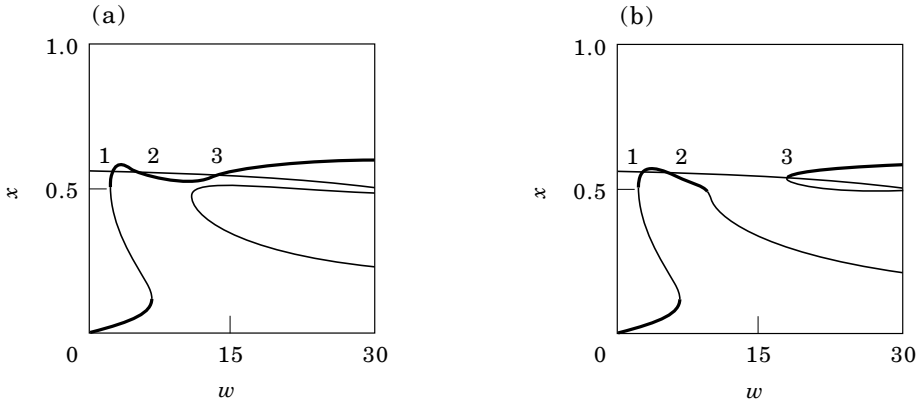

FIG. 3. Parameter region 6. The slow manifold and the w-nullcline (thin, nearly horizontal line) in the (w, x)-plane. The meaning of the bold lines is as in Fig. 2(a). There are five equilibrium points: 1 and 3 are stable and 2, 4 and 5 are unstable (equilibria 4 and 5 are not shown). (a) $p = 0.394$, $\epsilon = 0.56$. (b) $p = 0.4$, $\epsilon = 0.56$. At $p \approx 0.394$ and $\epsilon \approx 0.524$, a cusp bifurcation has occurred.

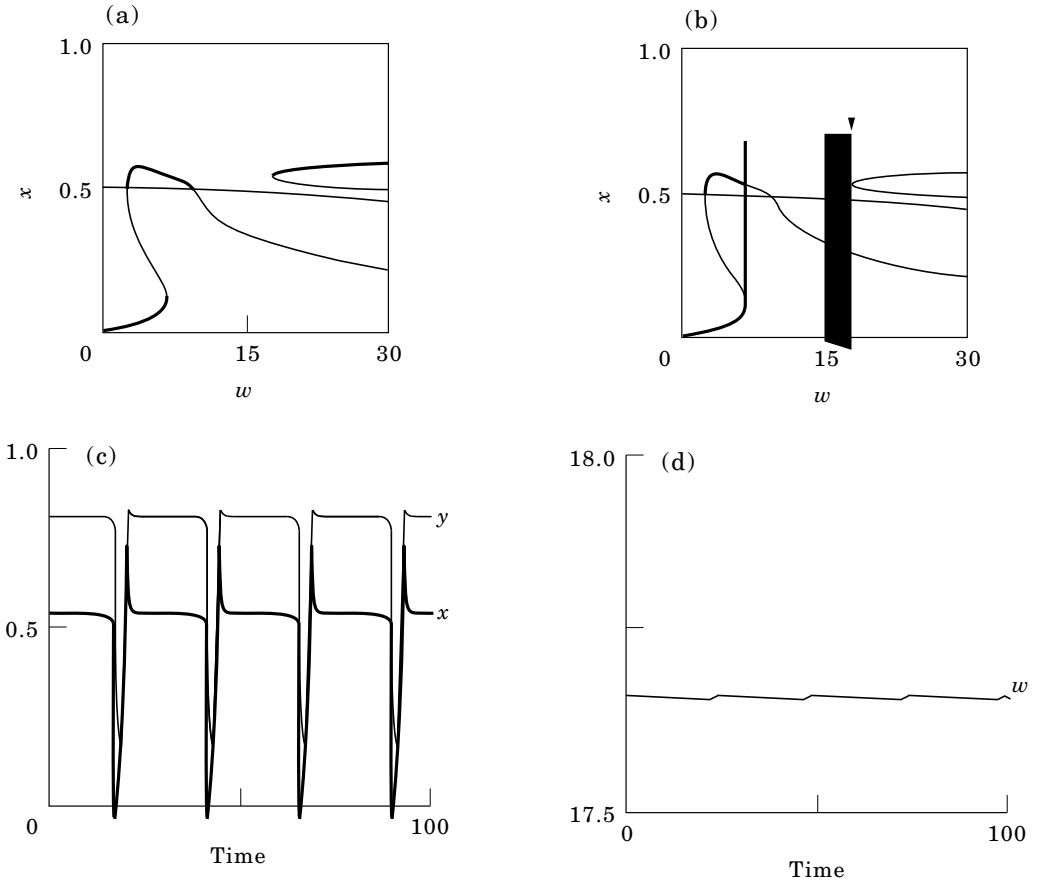

FIG. 4. Parameter region 5b: $p = 0.4$, $\epsilon = 0.5$. (a) The slow manifold and the w-nullcline (thin, nearly horizontal line) in the (w, x)-plane. The meaning of the bold lines is as in Fig. 2(a). (b) The slow manifold (without showing stability) and the w-nullcline in the (w, x)-plane. The bold lines are trajectories: one, starting at $w = 0$ and $x = 0$, approaches the point attractor at low w; the other one, starting at $w = 15$ and $x = 0$, approaches the limit cycle attractor (type 2) at $w \approx 17$ (see arrow). Starting at $w = 15$, x and y oscillate while w slowly increases until the oscillations "touch" the fold of the slow manifold, at which point there is no net increase in w anymore. At this point a homoclinic bifurcation occurs. Note that, since the changes in w are much slower than in x and y, the oscillations in x (and y) are so close together that they are not separately visible on this scale, and therefore appear as one vertical bar. (c) Time plot of the limit cycle attractor in (b) showing x (bold line) and y. (d) Time plot of the limit cycle attractor in (b) showing w.

Table 1

Region		Stable equation	Unstable equation	L.C. 1	L.C. 2	L.C. 3
1	a					0
	b	1	0	0	0	+
	c					0
2	a	0	1	1	0	0
	b				+	+
3		1	0	0	0	0
4	a	0	3	1	0	0
	b				+	+
5	a				0	0
	b	1	2	0	+	+
	c				0	−
6		2	3	0	0	0
7		1	4	0	+	−
8		0	1	0	0	+
9		2	1	0	0	0
10		2	1	0	0	−
11		1	2	0	+	−
12	a	2	1	0	0	−
	b					0
13	a	1	0	0	0	−
	b					0

The number and stability of equilibrium points in every region of the parameter plane shown in Fig. 1. The regions are divided into subregions, which have equal number and stability of equilibrium points, but differ in the presence of limit cycle attractors. "L.C. 1": limit cycle attractor of type 1, showing relaxation oscillations; "L.C. 2": limit cycle attractor of type 2, showing bursting oscillations; "L.C. 3": limit cycle attractor of type 3 " + ": this type of limit cycle exists at some points in the parameter region; " − ": the existence of this type of limit cycle cannot be excluded, but was not found; "0": this type of limit cycle or equilibrium point does not exist in the parameter region.

oscillate with a small amplitude, can make more oscillations before becoming trapped by the stable manifold of the saddle node [compare Fig. 5(b) and Fig. 5(d)]. In the other regions, in contrast, the amplitude of the oscillations of x and y is so large that they become immediately trapped by the stable manifold of the saddle node.

For the occurrence of a type 2 limit cycle, three conditions must be met: (i) an oscillatory state for x and y, which exists only for $0.39 < p < 0.77$ (for a fixed w); (ii) the existence of the homoclinic bifurcation; and (iii) a net increase of w if $w < w_{homoclinic}$, and a net decrease if $w > w_{homoclinic}$, where $w_{homoclinic}$ is the value of w at which the homoclinic bifurcation occurs. Because of these conditions, the type 2 limit cycle can exist only in parameter regions 2b, 4b, 5b, 7 and 11, although not everywhere in these regions, depending on whether or not condition (iii) is met. In all these regions, there exists another attractor in addition to the type 2 limit cycle (if present).

PARAMETER REGION 4B: TWO LIMIT CYCLE ATTRACTORS, ONE OF TYPE 1 AND ONE OF TYPE 2

In region 4, there are three unstable equilibrium points (Fig. 6) and a stable limit cycle of type 1. If the three conditions summed up in the previous paragraph are met, there also exists a limit cycle attractor of type 2. The two limit cycles show quite different dynamics. In the type 1 limit cycle, x, y and w oscillate very slowly with a high amplitude [Fig. 2(c, d)]. In contrast, the type 2 limit cycle in this region consists of a single, fast oscillation in x and y, and a longer phase with high steady activity, while w is virtually constant throughout the process [Fig. 4(c, d)].

PARAMETER REGION 1B: ONE POINT ATTRACTOR, ONE LIMIT CYCLE ATTRACTOR OF TYPE 3

In region 1 there is only one point attractor [see Fig. 7(a)]. At some places in this region there exists also a limit cycle attractor (which we will call a "type 3" limit cycle) [Fig. 7(b–d)]. This limit cycle, with fast oscillations in x and y, seems to be suspended at a certain value of w [Fig. 7(b)]. Intuitively, we can understand its existence as follows. For the parameter values used in Fig. 7, x and y will oscillate when $w > 7$. For w not too large, $x < (\epsilon - bw^2)$, on average, so that w will increase. However, at $w = 50$, for instance, $x > (\epsilon - bw^2)$, on average, so that w will decrease. Somewhere in between, therefore, there must be a value of w for which x, on average, equals $(\epsilon - bw^2)$, as a result of which no net increase or decrease in w will occur. Thus, a stable limit cycle exists, which shows oscillations with relatively high amplitude in x and y and low amplitude in w. In mathematical terms, we think that this limit cycle is born at a Hopf bifurcation on the Hopf line that is the boundary between region 1b and 2b. We could not define the conditions for the existence of the type 3 limit cycle as sharply as those for the type 2 limit cycle. It is found in regions 1b, 2b, 4b, 5b, 8. Note that the maximum number of attractors found in the whole parameter plane (ϵ, p) is two.

SUMMARY

In quite a number of parameter regions, two attractors exist (i.e., bistability), which can be either points attractors or limit cycles. The maximum number of attractors found in the whole parameter plane is two. The limit cycles can be classified into three types: one with regular, slow oscillations (type 1 or relaxation oscillations); one with regular, fast oscillations (type 3); and one with intermittent behaviour (type 2 or bursting oscillations): a relatively

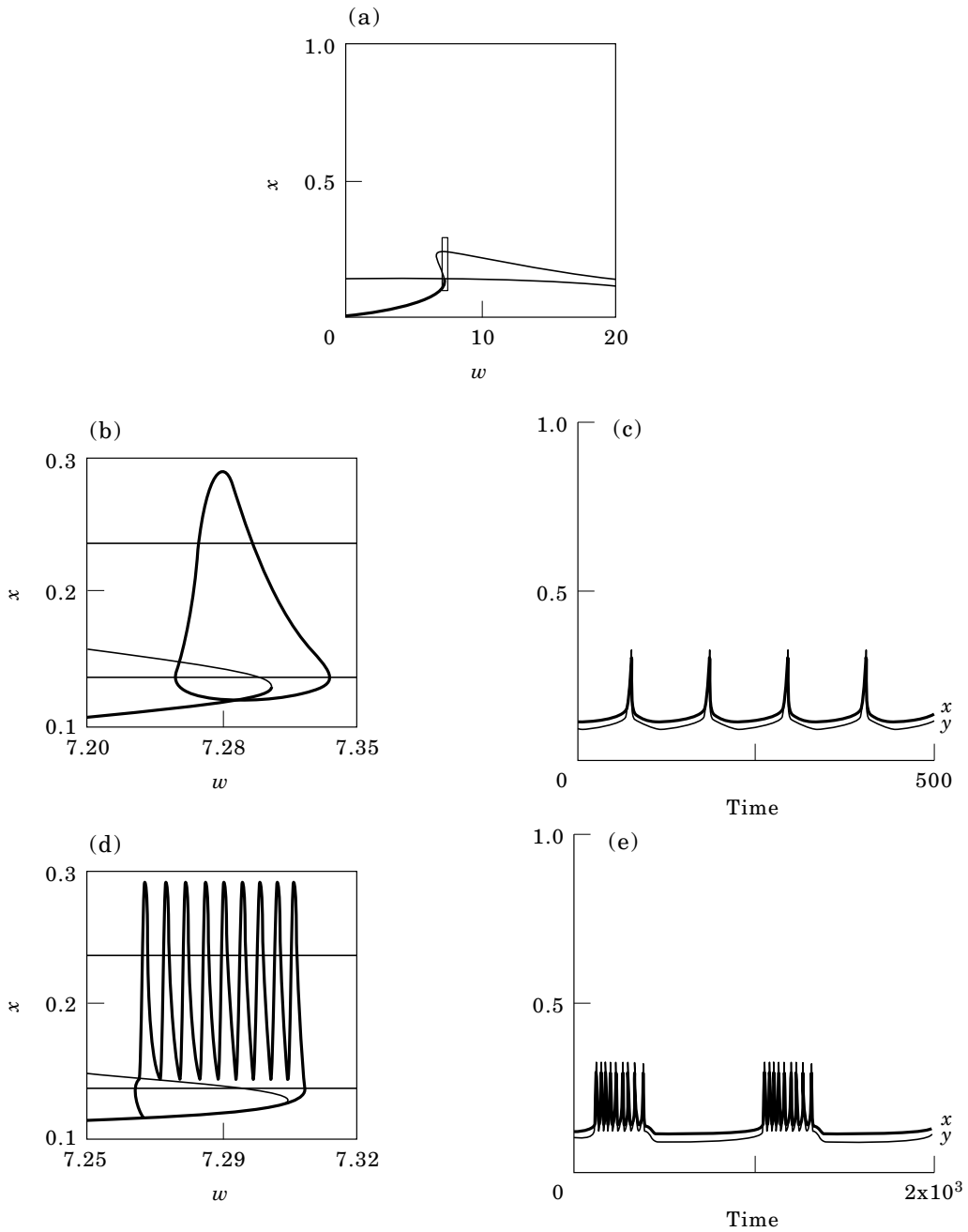

FIG. 5. Parameter region 2b: $p = 0.7$, $\epsilon = 0.14$ (a) The slow manifold and the w-nullcline (thin, nearly horizontal line) in the (w, x)-plane. The meaning of the bold lines is as in Fig. 2(a). The rectangle indicates the part that is enlarged in (b). (b) Enlargement of a part of the slow manifold together with the trajectory of the limit cycle attractor (type 2). Parameter $q = 0.1$. (c) Time plot of the limit cycle attractor in (b) showing x (bold line) and y. (d) Same as in (b), but with $q = 0.005$. (e) Time plot of the limit cycle attractor in (d) showing x (bold line) and y.

long phase with a steady activity level, alternating either with a single, fast oscillation or with a sequence of fast oscillations (see Figs 4 and 5). In many cases in which bistability is found, there is a point attractor (A) at a low value of w (and intermediate values of x and y) and another attractor (B) at a high value of w (see Figs 3, 4, 6 and 7). Attractor B can be either a point attractor or a limit cycle of type 2 or 3.

The initial conditions of the network determine which of these attractors will be reached. A trajectory starting at $w = 0$ (which is a normal initial condition for developing neurons) will approach attractor A in most cases. A trajectory starting at high enough

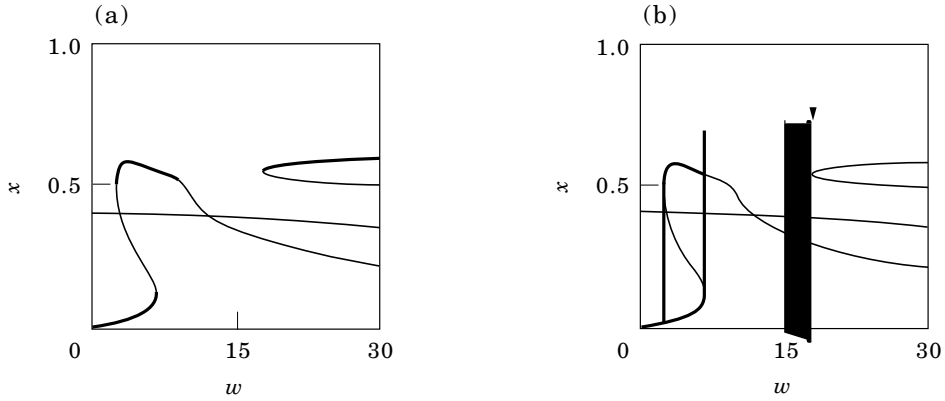

FIG. 6. Parameter region 4b: $p = 0.4$, $\epsilon = 0.4$. (a) The slow manifold and the w-nullcline (thin, nearly horizontal line) in the (w, x)-plane. The meaning of the bold lines is as in Fig. 2(a). (b) The slow manifold (without showing stability) and the w-nullcline in the (w, x)-plane. The bold lines are trajectories: one, starting at $w = 0$ and $x = 0$, approaches the limit cycle attractor of type 1 (relaxation oscillations); the other one, starting at $w = 15$ and $x = 0$, approaches the limit cycle attractor of type 2 at $w \approx 17$ (see arrow), in the same way as described for Fig. 4(b). Note that, since the changes in w are much slower than in x and y, the oscillations in x (and y) are so close together that they are not separately visible on this scale, and therefore appear as one vertical bar.

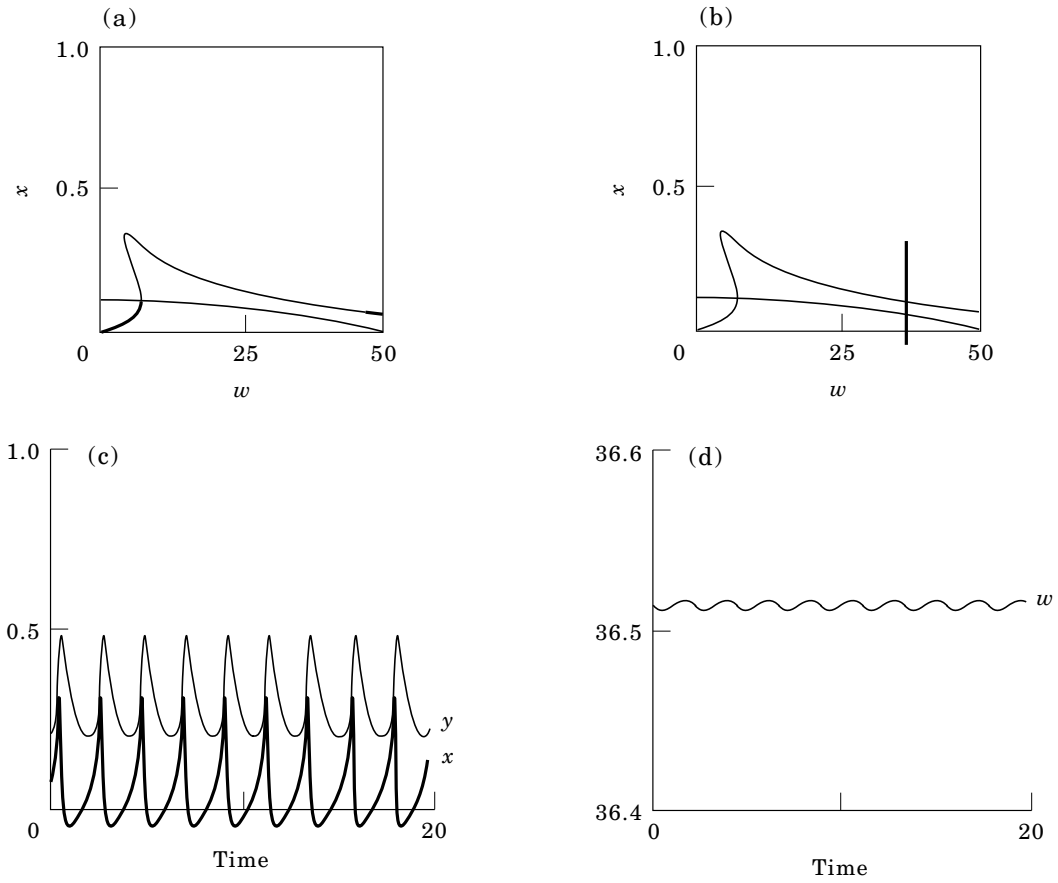

FIG. 7. Parameter region 1b: $p = 0.6$, $\epsilon = 0.12$. (a) The slow manifold and the w-nullcline in the (w, x)-plane. The meaning of the bold lines is as in Fig. 2(a). (b) The slow manifold (without showing stability) and the w-nullcline in the (w, x)-plane. The bold line is the trajectory of the type 3 limit cycle attractor (no initial transients are shown). (c) Time plot of the limit cycle attractor in (b) showing x (bold line) and y. (d) Time plot of the limit cycle attractor in (b) showing w.

values of w, however, will approach attractor B. At a value of w in between those of the two attractors, there must exist an unstable node or unstable limit cycle, forming the boundary between the basins of attraction of both attractors. For example, let us consider a parameter setting with $p < 0.77$, so hysteresis is present [see Fig. 4(a, b)]. Starting at $w = 0$, the trajectory moves along the lower branch of the S-shaped slow manifold and then jumps to the upper branch. This transition is the onset of high electrical activity. Let us call the value of w at which this transition occurs $w_{transition}$, and the value of w at which the unstable node or limit cycle exists $w_{critical}$. Then, starting at $w = 0$, attractor A is reached if $w_{transition} < w_{critical}$, and attractor B if $w_{transition} > w_{critical}$. In general, the higher p and ϵ, the lower $w_{critical}$, while $w_{transition}$ appears to be almost independent of p (and independent of ϵ). For higher values of p ($p > 0.43$) this means that for most ϵ values even the initial condition $w = 0$ is in the basin of attraction of B (see Fig. 8).

When electrical activity is chronically blocked in the model (analogous to the "critical" period experiment described in the Introduction) until w has become higher than $w_{critical}$, the system will approach attractor B rather than A when electrical activity is allowed to return.

Switching from one attractor to the other can be accomplished by changing either w, x or y. To switch from attractor A to B we need either to increase w, to chronically increase y, or to chronically decrease x. The opposite changes are required to switch from B to A.

Parameter q determines the time-scale of the slow connectivity changes. Changing the value of q over a range of $[1 \cdot 10^{-5}, 2]$ does not alter the stability nor the location of the attractors. However, as mentioned earlier, it can influence the dynamic behaviour of the type 2 limit cycle in parameter regions 2b and 11. Furthermore, if q is increased, the amplitude of the oscillations in w of the type 3 limit cycle increases.

4. Neurite Outgrowth of Both Cell x and Cell y

In the previous model, the connection strengths between the cells (i.e., w and pw) are modulated by the electrical activity of cell x only, as R_y was taken to be constant. This simplified model can already yield behaviour as was observed in the network model [see Introduction and van Ooyen *et al*. (1995)]. Nevertheless, it would be interesting to see whether the behaviour of the model is affected when R_y too is modulated by the electrical activity (as in the network model). We therefore made a start at the analysis of a model in which R_y is not constant, so that w_{xy} becomes a function of both R_x and R_y. Again taking simple functions for φ and ψ, we have:

$$\begin{aligned} w_{xx} &= a^* R_x S_{xx} \\ w_{xy} &= a^* \frac{R_x + R_y}{2} S_{xy}, \end{aligned} \tag{6}$$

which can be rewritten into:

$$\begin{aligned} w_{xx} &= a R_x \\ w_{xy} &= ap \frac{R_x + R_y}{2}, \end{aligned} \tag{7}$$

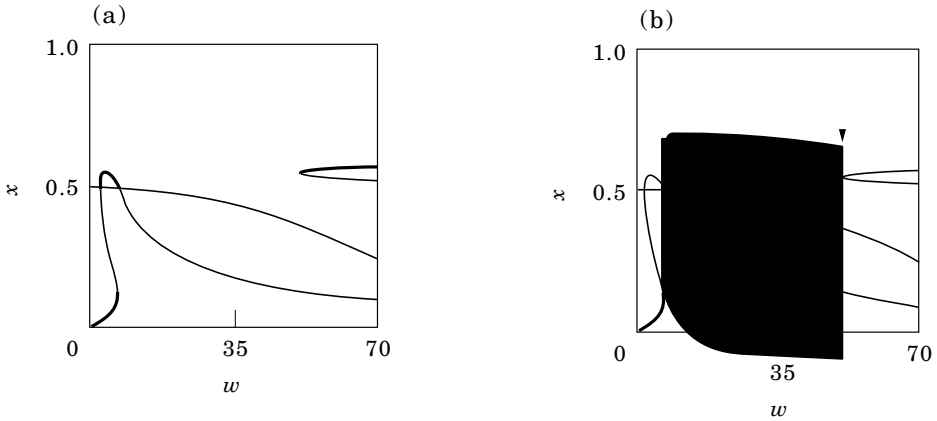

FIG. 8. For e.g., $p = 0.42$, $\epsilon = 0.5$, the initial condition ($w = 0$, $x = 0$) is in the basin of attraction of attractor B (here a limit cycle of type 2, see arrow). (a) The slow manifold and the w-nullcline in the (w, x)-plane. The meaning of the bold lines is as in Fig. 2(a). (b) The slow manifold (without showing stability) and the w-nullcline in the (w, x)-plane. The bold line is a trajectory starting at $w = 0$ and $x = 0$; x and y oscillate while w slowly increases until the oscillations "touch" the fold of the slow manifold, at which point there is no net change in w anymore. Note that, since the changes in w are much slower than in x and y, the oscillations in x (and y) are so close together that they are not separately visible on this scale, and therefore appear as one vertical bar.

where

$$a = a^* S_{xx}$$

$$p = S_{xy}/S_{xx}.$$

Here $\psi(R_x, R_y)$ is simply a linear function of the neuritic field sizes. Studies in comparable models have indicated that the results are not much affected by the actual choice of $\psi(R_x, R_y)$ and $\varphi(R_x)$ (e.g., $\varphi(R_x) \sim R_x^2$ and $\psi(R_x, R_y) \sim R_x R_y$) (van Ooyen & van Pelt, 1995). The full model consists of eqns (1), (2) and (7), and will be called the "extended model". Again, we take $w_{yy} = 0$ and $w_{yx} = w_{xy}$. The parameter values used are: $\theta = 0.5$, $\alpha = 0.1$, $h = 0.1$, $q^* = 5 \cdot 10^{-3}$, $b^* = 5 \cdot 10^{-5}$, $a = 1$. The parameters p and ϵ vary from 0 to 1; their exact values are denoted in the figures.

Preliminary results show that most of the behaviour found in the basic model is also present in the extended model. For low values of p ($p < 0.25$), a stable equilibrium point exists for $\epsilon < 0.12$, just as in parameter region 1 of the basic model. At intermediate values of ϵ ($0.12 < \epsilon < 0.5$), a limit cycle of type 1 exists [see Fig. 9; compare Fig. 2(c, d)]. If $\epsilon > 0.5$, there is again a stable equilibrium, and a trajectory starting at $R_x = R_y = 0$ shows overshoot with respect to w_{xx} and w_{xy} (region 3 in the basic model). Bistability is found for various parameter settings. In all these cases, there is a point attractor where w_{xx} and w_{xy} are smaller than 10 (attractor A), and a limit cycle attractor, where x, y, w_{xx} and w_{xy} oscillate with high amplitude (since the average values of w_{xx} and w_{xy} are larger than those in the point attractor, we call this attractor B, in analogy to the basic model). Which of these attractors will be approached is highly dependent on the initial conditions, as shown in Fig. 10: a trajectory starting at $R_x = R_y = 0$ approaches the point attractor [Fig. 10(a, b)], whereas one starting at $15 \leqslant R_x = R_y < 28$ approaches the limit cycle attractor [Fig. 10(c, d)]. New compared to the basic model is that trajectories starting at even higher connectivity values ($R_x = R_y \geqslant 28$) approach the point attractor once again. Obviously, the asymptotic behaviour of the extended model is much more difficult to predict from the initial conditions than the asymptotic behaviour in the basic model.

Also, the transient behaviour in the extended model is more complex than in the basic model. The trajectories often show transient oscillations before ending up in an attractor. Such behaviour is also found in the network model (van Ooyen *et al*., 1995) but is scarcely present in the basic model. In addition, the limit cycle attractor has much more complex dynamics than any limit cycle in the basic model [Fig. 10(c)].

Similar to the basic model is that for low values of p ($p < 0.43$) and for most values of ϵ, trajectories starting at $R_x = R_y = 0$ approach attractor A, whereas for high values of p they approach attractor B.

5. Generalization

In the previous sections we have considered neurite outgrowth as an example of a relatively slow, activity-dependent process that attempts to stabilize neuronal activity by adapting a cellular property. Another example of such a general process is postsynaptic receptor adaptation. After prolonged exposure to its neurotransmitter, for example, a receptor may become desensitized (Schwartz & Kandel, 1991). Also the number of receptors can be regulated, with down-regulation generally following an increase, and up-regulation following a decrease in electrical activity. In the following, we describe a

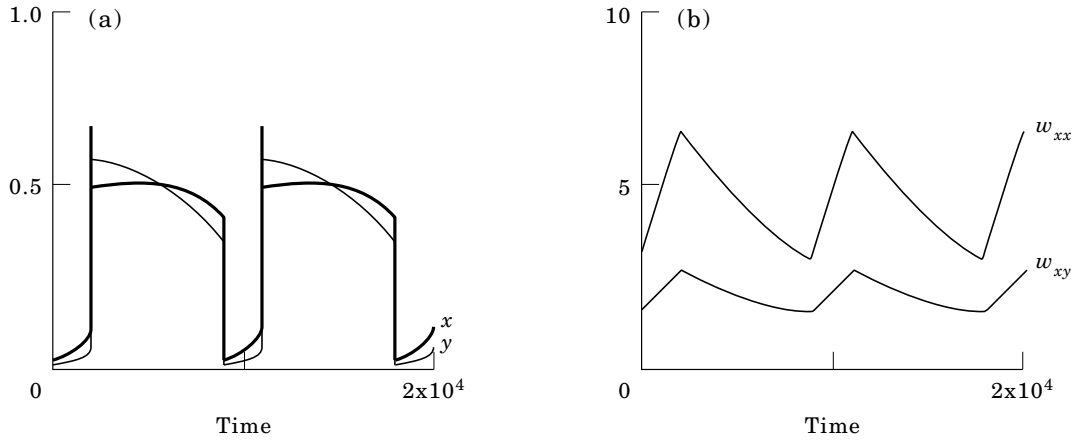

FIG. 9. Time plots of a type 1 limit cycle attractor in the extended model. $p = 0.3$, $\epsilon = 0.4$. (a) x (bold line) and y; (b) w_{xx} and w_{xy}.

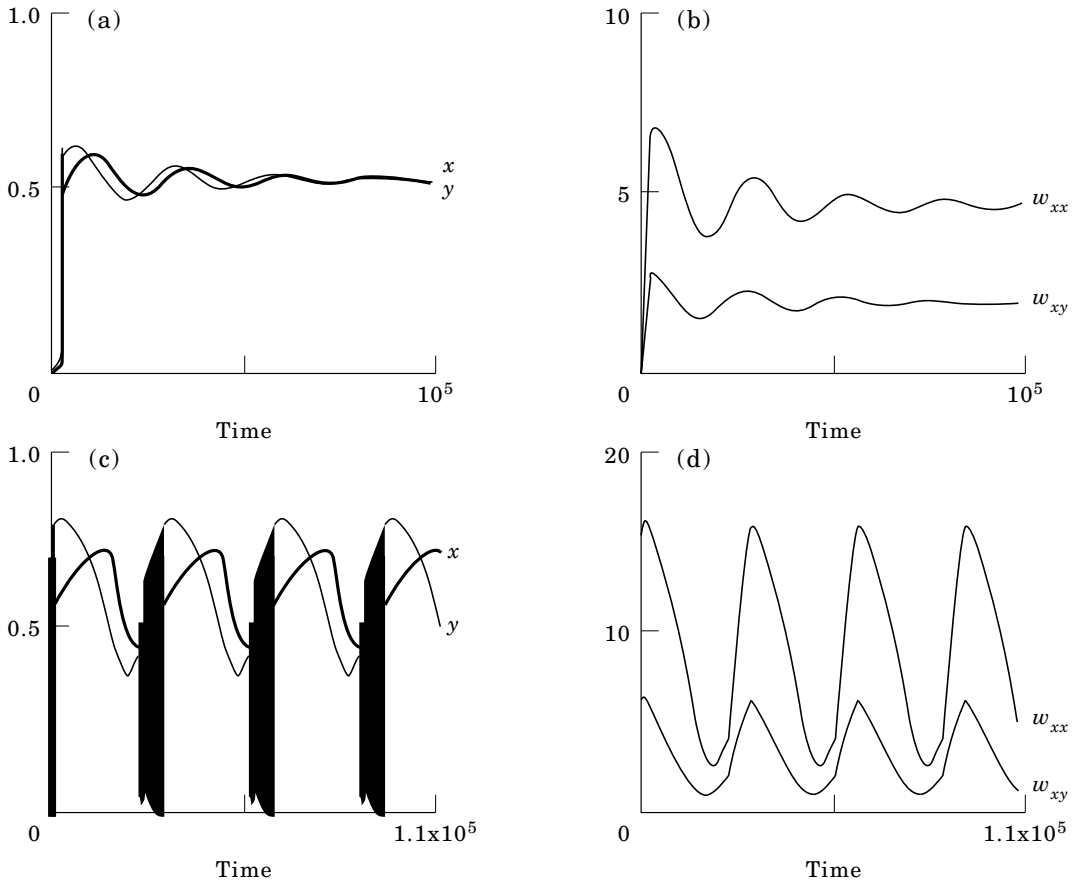

FIG. 10. Sensitivity to initial conditions in the extended model. $p = 0.41$, $\epsilon = 0.54$. For initial condition $x = y = R_x = R_y = 0$, the trajectory approaches the point attractor: (a) x (bold line) and y; (b) w_{xx} and w_{xy}. For initial condition $x = y = 0$; $R_x = R_y = 15.0$, the trajectory approaches the limit cycle attractor: (c) x (bold line) and y; (d) w_{xx} and w_{xy}.

two-cell model, in which the receptor number/sensitivity of the postsynaptic cell adapts to the cell's membrane potential. For the connection strengths between the cells we have:

$$\begin{aligned} w_{xx} &= r_x s_{xx} = w_x \\ w_{xy} &= r_x s_{xy} = p w_x \\ w_{yx} &= r_y s_{yx} = w_y, \end{aligned} \tag{8}$$

where $p = s_{xy}/s_{xx}$; s_{xx}, s_{xy} and s_{yx} are constants representing the number of connections (or presynaptic connection strength) from cell x to x, y to x and x to y, respectively (all $s > 0$); r_x and r_y are variable, e.g., representing the effectiveness of the receptors of x and y, respectively ($r_x > 0$ and $r_y > 0$). In general, r_x and r_y represent any intrinsic (postsynaptic) cellular property that determines the effectiveness of all the cell's incoming connections. Thus, the strength of all the connections onto a cell is regulated by the postsynaptic cell only. Note that in contrast with the previous two models, $w_{xy} \neq w_{yx}$ [see eqns (1) and (5)].

Analogous to the models describing neurite outgrowth, the dynamics of r_x and r_y are given by:

$$\begin{aligned} \frac{dr_x}{dt} &= q^*(\epsilon - b^* r_x^2 - x) \\ \frac{dr_y}{dt} &= q^*(\epsilon - b^* r_y^2 - y), \end{aligned} \tag{9}$$

where q^* determines the rate of change in r_x and r_y, and b^* the degree of saturation. As in eqn (2), the term $-b^* r_u^2$ prevents r_u from ever increasing indefinitely. Note that in eqn (8) we took the same variable, r_x, for the receptors in the excitatory and inhibitory connections, so that the excitatory cell changes the strength of its incoming excitatory connection (w_x) in the same way as the strength of its incoming inhibitory connection (pw_x). The assumption is that the receptors of both the inhibitory neurotransmitter (e.g., GABA) and of the excitatory neurotransmitter (e.g., glutamate) increase their efficacy at low x, and decrease it at high x. Indeed, the number of AMPA receptors (a glutamate receptor

sub-type) has been found to decrease as a result of increased neuronal activity (Shaw & Lanius, 1992). Also a decreased GABA receptor function due to activity-dependent calcium influx has been found (Stelzer & Shi, 1994). Conversely, the efficacy of both GABA and glutamate receptors have been shown to increase as a result of chronically blocking electrical activity (Ramakers *et al*., 1994).

In analogy with eqn (5), we have studied the case in which r_y is constant. Thus, the full model becomes [combining eqns (8) and (9)]:

$$\frac{dx}{dt} = -x + (1-x)w_x f(x) - (h+x)w_x p f(y)$$

$$\frac{dy}{dt} = -y + (1-y)w_y f(x) \qquad (10)$$

$$\frac{dw_x}{dt} = q(\epsilon - bw_x^2 - x),$$

where

$$q = s_{xx}q^*$$

$$b = b^*/s_{xx}^2$$

This model will be referred to as the "receptor model". An interpretation of eqn (10) in terms of neurite outgrowth would be that only the dendrites of the excitatory cell grow out in an activity-dependent manner, while the axons do not react to electrical activity, and thus remain at a certain size. The parameter values used are the same as those in the model defined by eqn (5). Although the shape of the slow manifold is different from that in the basic model, the dynamic behaviour is still similar. Bistability can be found, with a point attractor at a low value of w_x, and a limit cycle attractor of type 3 at a higher value of w_x (Fig. 11). A trajectory from the initial condition $w_x = 0$ approaches the point attractor, whereas a trajectory from an initial condition $w_x \geqslant 8.0$ approaches the limit cycle attractor. In analogy with the results of the extended model, we

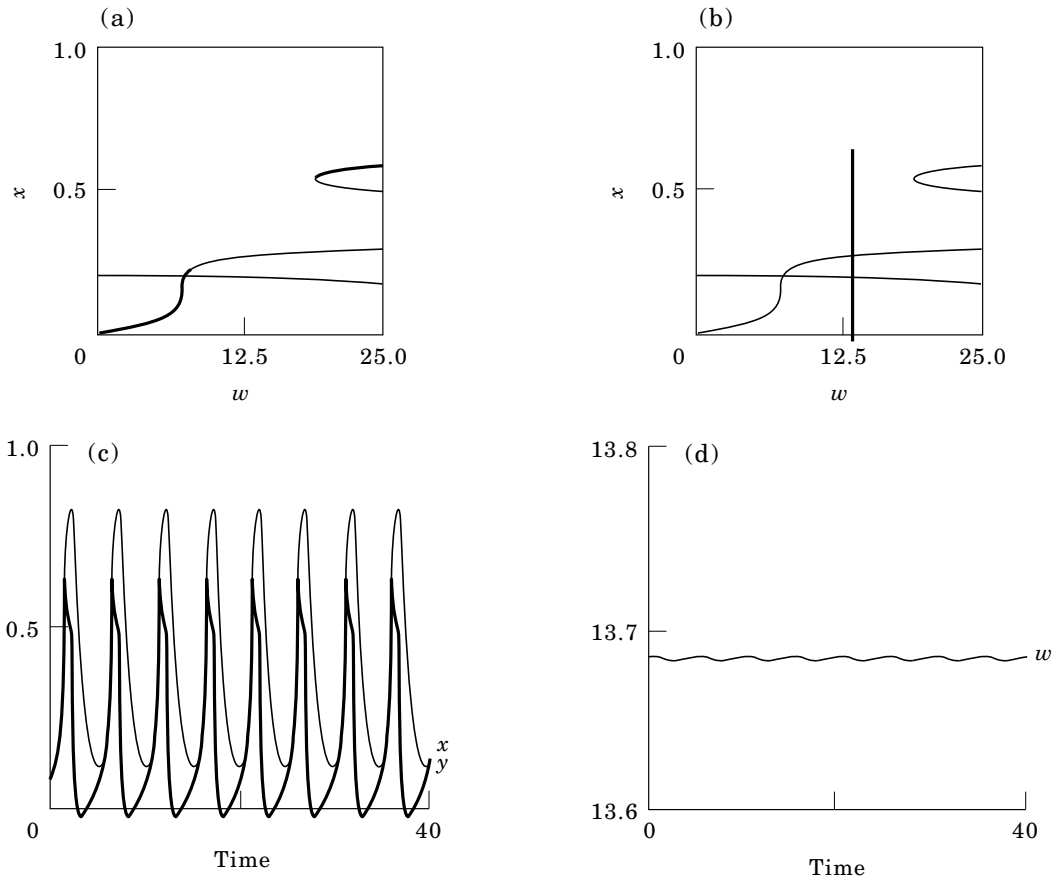

FIG. 11. Bistability in the receptor model. $p = 0.35$, $\epsilon = 0.2$, and $w_y = 8$. (a) The slow manifold and the w-nullcline (thin, nearly horizontal line) in the (w, x)-plane. The meaning of the bold lines is as in Fig. 2(a). (b) The slow manifold (without showing stability) and the w-nullcline in the (w, x)-plane. The bold line is the trajectory of the type 3 limit cycle attractor (no initial transients are shown). (c) Time plot of the limit cycle attractor in (b) showing x (bold line) and y. (c) Time plot of the limit cycle attractor in (b) showing w.

expect that multistability will still be present if w_y too is made activity-dependent.

6. Discussion

In this paper we have shown that a simple, activity-dependent neurite outgrowth rule, in combination with inhibition, can generate extremely rich dynamic behaviour. The models which we used were very much simplified: in our "basic model" [eqn (5)], two cells were considered, of which only the excitatory cell could adapt its neurites under influence of its own activity. This enabled us to systematically study the complete repertoire of dynamic behaviour. Despite the simplifications, this model appears to capture the essential interactions necessary for generating two important properties of the much more complicated "network model" [see Introduction and van Ooyen *et al*. (1995)]. These properties of the network model are (i) overshoot with respect to connectivity, and (ii) the "normal" attractor at low connectivity is not approached under all initial conditions; more specifically, if the initial level of connectivity exceeds a critical value, connectivity will not decrease, but instead increases still further.

In the network model, in contrast to the basic model, an attractor at high connectivity has not been found: the connectivity just continues to increase (van Ooyen *et al*., 1995). The specific description of neuritic fields as circles in the simulation model may account for this difference, since the equivalence between both models is worse at high connectivity. In addition, the equation for the outgrowth of neuritic fields in the network model does not contain a saturation term (which is, of course, biologically implausible). Introducing a saturation term would obviously create an attractor at high connectivity, since neuritic fields can then no longer grow out without bound (in the basic model such an attractor occurs also without a saturation term, see below).

The most important properties of the basic model (namely bistability along with point and limit cycle attractors) are retained in the model with neurite adaptation of both the excitatory and inhibitory cell (the "extended model"), as well as in the modified model ("receptor model"). With the latter model a new range of activity-dependent processes could be described. These are processes whereby a postsynaptic cellular property that determines the efficacy of the incoming connections, is modulated by the cell's own level of electrical activity (an example of such a process is postsynaptic receptor adaptation). What all these models have in common is that a neuron attempts to reach and maintain a given level of its electrical activity ("homeostasis"), whereby the adaptational changes in the connections from the inhibitory and excitatory units to this neuron are somehow coupled. Thus, for example, when a neuron increases the size of its neurites because the level of activity is too low, more input will be received from both excitatory and inhibitory cells. This seems biologically plausible. In the case of uniform changes in receptor sensitivity, both glutamate receptors and GABA receptors become more sensitive. This has indeed been reported in a number of studies on receptor function (see Section 5).

Note that these homeostatic processes, where a neuron tries to maintain a given level of electrical activity, are different from the Hebbian rule, which, in contrast, modifies electrical activity, by increasing the connection strength between two neurons when they are simultaneously active.

To investigate whether saturation is essential for our results, we removed the saturation terms in eqns (2), (5), (9) and (10). Limit cycles of type 1, 2 and 3 are still found. Without saturation, there is only one attractor in some parameter regions. Either this attractor is approached, or the connection strength increases indefinitely. In various other parameter regions, however, the two attractors are still present. Whether there are two attractors or not, the attractor that is reached when the system starts at low connectivity, is not reached when the initial connectivity exceeds a critical value. Thus saturation is not essential for this phenomenon.

Since our aim in this study was not to investigate the implications of saturation per se, the effects of different values of b were not investigated systematically. Small changes in b do not affect the results, but if b is of the order 10^{-2}, the results can become different. For example, at $b = 3 \cdot 10^{-2}$, $p = 0$ and $\epsilon = 0.7$, the w-nullcline intersects the slow manifold three times. This results in two stable equilibrium points, whereas for lower b there exists only one equilibrium point.

COMPARISON WITH EMPIRICAL DATA

In comparing the model results with empirical findings, one should keep in mind that the model results are not much affected by changes in q, the parameter determining the rate of change of the adaptational process (e.g., neurite outgrowth or receptor sensitivity). The activity-dependent process implemented in the model could thus stand for a range of such processes that may operate on different time scales. In this discussion, we will consider activity-dependent processes on a time-scale of days

or weeks, and those on a time-scale of hours. They include developmental processes as well as processes operating in adulthood. In comparing the model with experiments, one should further realize that individual action potentials are not modelled but, rather, firing rates (and, therefore, time averaged membrane potentials). A high value of x [and, consequently, $f(x)$] stands for a high firing rate of the excitatory cell over a certain period of time. A steady activity level represents a firing rate that does not alter significantly over time, which does not necessarily imply that the neurons fire regularly. Thus, an oscillation of type 2 as shown in Fig. 5(c) consists of short phase during which many action potentials are generated (''bursts'') and a longer quiescent phase. An oscillation as shown in Fig. 5(e) consists of a long quiescent phase and a phase during which bursts are separated by very short relative silent intervals.

''Critical'' period

When electrical activity is chronically blocked, developing cultures of dissociated cerebral cortex cells show enhanced neurite outgrowth and a persistence of a high density of synapses (van Huizen & Romijn, 1987; also see Introduction). If then placed in control medium, the electrical activity rapidly returns, although there is no subsequent elimination of the excess synapses.

These results have been taken as suggestive that a ''critical'', or ''sensitive'', period exists after which electrically controlled elimination of synapses is no longer possible (van Huizen *et al*., 1987b). Although the intrinsic properties of the cells in the model do not change over time (as they might well do in the living system), the interactions between excitation, inhibition and outgrowth are nevertheless capable of generating similar phenomena. In the basic model, trajectories starting at the normal initial condition $w = 0$ end up [if the relative strength of the inhibitory connection (p) is not too high] in the attractor at low connectivity (attractor A). Blocking electrical activity for longer than a certain period, so that the connectivity w becomes higher than a critical value, causes the system to end up in the attractor at high connectivity (attractor B) when electrical activity is allowed to return.

In the above mentioned experiments with dissociated cortex cells, abnormal or ''pathological'' conditions (such as chronically blocking electrical activity) lead to a state with a persistence of a high density of synapses. In the model this state corresponds to attractor B, which suggests that attractor A would represent the end state of a ''normally'' developed network, whereas attractor B would represent the end state of a ''pathologically'' developed network. This interpretation is further supported by comparing the activity patterns in the attractors with those found in culture. Cells whose electrical activity has been blocked during development have significantly altered activity patterns in comparison with normally developed cells, the main difference being the enhanced ''bursting'' pattern of the former (Corner & Ramakers, 1992). This supports the pathological nature of attractor B, the activity pattern of which is indeed burst-like in some parameter regions.

Balance of excitation/inhibition

In all models, switching from attractor A to B can be accomplished either by increasing w (or R_x) or y, or, alternatively, by decreasing x. The switch from B to A requires one of the opposite modifications. In the receptor model, this switch would be relatively fast, since changes in receptor sensitivity can take place at a time-scale from minutes to hours. The model may also have relevance, therefore, for phenomena that occur on that time-scale, for example epilepsy. An epileptic seizure may be viewed as a sudden switch from one state of the network to another (e.g., Lopes da Silva *et al*., 1994). If we maintain our interpretation of A being a ''normal'', and B a ''pathological'' state of the network, a switch from A to B might represent an epileptic seizure. Interestingly, it is not a lack of inhibitory activity in this case that makes possible the seizure, but rather an excess. A recovery from the attack, i.e., a switch from B to A, would be attained by enhancing excitatory activity. This as a result of the neuronal adaptational processes taking place in response to electrical activity, which underlines the relevance of such processes for understanding epilepsy.

An important parameter in the nervous system is the balance between excitation and inhibition. Roughly defined, this is the ratio of excitatory to inhibitory elements (abbreviated as E/I), which includes the total number of excitatory and inhibitory cells, and the number and strength of their synapses. In the models, a high p corresponds to a low E/I. For all models, it holds that for a high p, a trajectory starting at $w = 0$ will reach attractor B. Thus, a network developing under conditions of relatively high inhibition with, for the rest, normal conditions will end up in the ''pathological'' state with oscillatory activity. In contrast, a low level of inhibition during the initial stage of development would enable the system to move to the normal state. Interesting in this regard is that during the development of the nervous system, the normally inhibitory neurotransmitter

GABA initially works in an excitatory fashion (Cherubini *et al*., 1991). One could thus hypothesize that this is so in order to reduce the risk of pathological development.

A number of recent experiments are in agreement with the above. Induced hypoxic-ischemic encephalopathy (HIE, i.e., brain damage a result of lack of oxygen) in rat pups can lead to permanent epileptiform activity later on in adulthood (Romijn *et al*., 1994a). HIE may result in an unstable cortical network generating abnormal oscillations in electrical activity (of both excitatory and inhibitory cells) which can be amplified and propagated as true epileptic discharges (Romijn *et al*., 1994b). Contrary to the authors' expectations, such epileptiform activity was not the result of a preferential loss of inhibitory elements following HIE, i.e., GABAergic cell bodies (Romijn *et al*., 1992) or GABAergic nerve endings (Romijn *et al*., 1993) in the damaged cerebral cortex. In fact the data show that there was a preferential survival of GABAergic nerve endings (an effect that was directly proportional to the severity of the incurred damage) and a higher proportion of GABA-immunoreactive neurons in the damaged areas. In interpreting these experiments with respect to the model, it is unimportant whether or not one assumes the system already to be in attractor A before HIE is induced, or still developing towards either attractor A or B. A higher p, as possibly induced by HIE, increases the size of the basin of attraction of B, so that: (i) when the system is still developing, the system is more likely to end up in B; or (ii) if the system is already in A, the decrease in electrical activity following HIE (e.g., Duffy & Plum, 1981), and the subsequent adaptational process, could switch the system to B. Since attractor B is at a higher connectivity w (but, of course, at the same p, since p is not a variable in the basic model) a prediction of the model is that in rats in which HIE has been induced, the total number of excitatory *and* inhibitory elements in adulthood will be larger than in control rats.

We thank M. A. Corner, J. van Pelt and F. H. Lopes da Silva for critically reading the manuscript.

REFERENCES

Carpenter, G. A. & Grossberg, S. (1983). A neural theory of circadian rhythms: the gated pacemaker. *Biol. Cybern.* **48,** 35–59.

Cherubini, E., Gaiarsa, J. L. & Ben-Ari, Y. (1991). Gaba: an excitatory transmitter in early postnatal life. *Trends Neurosc.* **14,** 515–519.

Cohan, C. S. & Kater, S. B. (1986). Suppression of neurite elongation and growth cone motility by electrical activity. *Science* **232,** 1638–1640.

Corner, M. A. (1994). Reciprocity of structure-function relations in developing neural networks: the odyssey of a self-organizing brain through research fads, fallacies and prospects. In *The Self-Organizing Brain*: *From Growth Cones to Functional Neural Networks* (van Pelt, J., Corner, M. A., Uylings, H. B. M. & Lopes da Silva, F. H., eds), pp. 3–31. Amsterdam: Elsevier.

Corner, M. A. & Ramakers, G. J. A. (1992). Spontaneous firing as an epigenetic factor in brain development—physiological consequences of chronic tetrodotoxin and picrotoxin exposure on cultured rat neocortex neurons. *Dev. Brain Res.* **65,** 57–64.

De Boer, R. J. (1983). GRIND: GReat INtegrator Differential equations. Bioinformatics Group, Padualaan 8, 3584 CH Utrecht, The Netherlands.

Duffy, T. E. & Plum, P. (1981). Seizures, coma, and major metabolic encephalopathies. In: *Basic Neurochemistry* (Siegel, G. J., Albers, R. W., Agranoff, B. W. & Katzmann, R., eds), pp. 700–705. Boston: Little Brown and Company.

Edelstein-Keshet, L. (1988). *Mathematical Models in Biology*. 1st Edn. New York: Random House.

Fields, R. D. & Nelson, P. G. (1992). Activity-dependent development of the vertebrate nervous system. *Int. Review Neurobiol.* **34**, 133–214.

Grossberg, S. (1988). Nonlinear neural networks: principles, mechanisms and architectures. *Neural Networks* **1**, 17–61.

Hodgkin, A. L. & Huxley, A. F. (1952). A quantitative description of membrane current and its application to conduction and excitation in nerve. *J. Physiol.* **117**, 500–544.

Kater, S., Guthrie, P. & Mills, L. (1990). Integration by the neuronal growth cone: a continuum from neuroplasticity to neuropathology. *Progress in Brain Research* **86**, 117–128.

Khibnik, A., Kuznetsov, Y. A., Levitin, V. & Nikolaev, E. (1992). LOCBIF: Interactive LOCal BIFurcation Analyzer. CAN Expertise Centre, Kruislaan 413, 1098 SJ Amsterdam, The Netherlands, 2nd Edn.

Lopes da Silva, F. H., Pijn, J.-P. & Wadman, W. J. (1994). Dynamics of local neuronal networks: control parameters and state bifurcations in epileptogenesis. In: *The Self-Organizing Brain*: *From Growth Cones to Functional Neural Networks* (van Pelt, J., Corner, M. A., Uylings, H. B. M. & Lopes da Silva, F. H., eds), pp. 359–370. Amsterdam: Elsevier.

Mattson, M. P. (1988). Neurotransmitters in the regulation of neuronal cytoarchitecture. *Brain Res. Rev.* **13**, 179–212.

Ramakers, G., van Galen, H., Feenstra, M., Corner, M. & Boer, G. (1994). Activity-dependent plasticity of inhibitory and excitatory amino acid transmitter systems in cultured rat cerebral cortex. *Int. J. Devl. Neuroscience* **12**, 611–621.

Rinzel, J. & Ermentrout, G. (1989). Analysis of neural excitability and oscillations. In *Methods in Neuronal Modeling*: *From synapses to networks* (Koch, C. & Segev, I., eds), pp. 135–171. Cambridge, MA: The MIT Press.

Romijn, H. J., Janszen, A. W. J. W., van Voorst, M. J. D., Buijs, R. M., Balázs, R. & Swaab, D. F. (1992). Perinatal hypoxic ischemic encephalopathy affects the proportion of gaba-immunoreactive neurons in the cerebral cortex of the rat. *Brain Res.* **592**, 17–28.

Romijn, H. J., van Marle, J. & Janszen, A. W. J. W. (1993). Permanent increase of the gad_{67}/synaptophysin ratio in rat cerebral cortex nerve endings as a result of hypoxic ischemic encephalopathy sustained in early postnatal life: a confocal laser scanning microscopic study. *Brain Res.* **630**, 315–329.

Romijn, H. J., Voskuyl, R. A. & Coenen, A. M. L. (1994a). Hypoxic ischemic encephalopathy sustained in early postnatal life may result in permanent epileptic activity and an altered cortical convulsive threshold in rat. *Epilepsy Res.* **17**, 31–42.

Romijn, H. J., Janszen, A. W. J. W. & van Marle, J. (1994b). Quantitative immunofluorescence data suggest a permanently enhanced gad_{67}/gad_{65} ratio in nerve endings in rat cerebral cortex

damaged by early postnatal hypoxia-ischemia: a comparison between two computer-assisted procedures for quantification of confocal laser scanning microscopic immunofluorescence images. *Brain Res*. **657**, 245–257.

SCHWARTZ, J. H. & KANDEL, E. R. (1991). Synaptic transmission mediated by second messengers. In *Priciples of Neural Science* (Kandel, E. R., Schwartz, J. H. and Jessell, T. M., eds), pp. 173–193. Englewood Cliffs, LJ: Prentice-Hall.

SHAW, C. & LANIUS, R. A. (1992). Cortical ampa receptors: age-dependent regulation by cellular depolarization and agonist stimulation. *Devl*. *Brain Res*. **68**, 225–231.

STELZER, A. & SHI, H. (1994). Impairment of $GABA_A$ receptor function by *N*-methyl-D-aspartate-mediated calcium influx in isolated CA1 pyramidal cells. *Neurosci*. **62**, 813–828.

VAN HUIZEN, F. (1986). Significance of Bioelectric Activity for Synaptic Network Formation. PhD Thesis, University of Amsterdam.

VAN HUIZEN, F., ROMIJN, H. J. & HABETS, A. M. M. C. (1985). Synaptogenesis in rat cerebral cortex is affected during chronic blockade of spontaneous bioelectric activity by tetrodotoxin. *Dev*. *Brain Res*. **19**, 67–80.

VAN HUIZEN, F. & ROMIJN, H. J. (1987). Tetrodoxin enhances initial neurite outgrowth from fetal rat cerebral cortex cells *in vitro*. *Brain Res*. **408**, 271–274.

VAN HUIZEN, F., ROMIJN, H. J., HABETS, A. M. M. C. & VAN DEN HOOFF, P. (1987a). Accelerated neural network formation in rat cerebral cortex: cultures chronically disinhibited with picrotoxin. *Exp*. *Neurol*. **97**, 280–288.

VAN HUIZEN, F., ROMIJN, H. J. & CORNER, M. (1987b). Indications for a critical period for synapse elimination in developing rat cerebral cortex cultures. *Devl*. *Brain Res*. **13**, 1–6.

VAN OOYEN, A. (1994). Activity-dependent neural network development. *Network*, **5**, 401–423.

VAN OOYEN, A. & VAN PELT, J. (1994). Activity-dependent outgrowth of neurons and overshoot phenomena in developing neural networks. *J*. *theor*. *Biol*. **167**, 27–43.

VAN OOYEN, A. & VAN PELT, J. (1996). Complex periodic behaviour in a neural network model with activity-dependent neurite outgrowth. *J*. *theor*. *Biol*. **179,** 229–242.

VAN OOYEN, A., VAN PELT, J. & CORNER, M. (1995). Implications of activity-dependent neurite outgrowth for neuronal morphology and network development. *J*. *theor*. *Biol*. **172**, 63–82.

VAN OSS, C. & VAN OOYEN, A. (1995). Activity-dependent neurite outgrowth in a simple neural network model including excitation and inhibition. In *Artificial Neural Networks*, *Proc*. 3*rd European Symp*. *on Artificial Neural Networks* (Verleysen, M., ed.), pp. 87–92. Brussels: D facto.

WILSON, H. & COWAN, J. (1972). Excitatory and inhibitory interactions in localized populations of model neurons. *Biophys*. *J*. **12**, 1–24.